Asteroseismology: AI-Driven Seismic Event Detection for Extra-Terrestrial Missions

Muhammad Zain Ali
Dept. of Physics
Quaid-i-Azam University
Islamabad, Pakistan
zain@betelwise.com

Khabab Nazir
Dept. of Physics
Quaid-i-Azam University
Islamabad, Pakistan
khababnazir10@gmail.com

Abstract—Planetary seismology is crucial for understanding the internal structure and evolution of celestial bodies, but missions face severe data transmission limitations due to bandwidth and power constraints. Traditional onboard event detection methods often struggle with high false positive rates, leading to inefficient use of these limited resources. This paper introduces "Asteroseismology," an AI-enhanced hybrid framework designed to optimize seismic event detection for space missions. The framework first employs an Initial Processing and Candidate Selection (IPCS) stage, which utilizes conventional seismic algorithms. This includes adaptive bandpass filtering based on signal characteristics (power spectrum or standard deviation), outlier removal, normalization, and STA/LTA analysis for initial event triggering. A key refinement within this stage involves analyzing characteristic function slopes to reduce false STA/LTA detections. Candidate events from the IPCS stage are then passed to a Machine Learning-based Event Verification (MLEV) stage. Unlike approaches that primarily use 2D spectrograms, our MLEV stage utilizes 1D seismogram segments augmented with explicitly engineered auxiliary statistical features (standard deviations around the arrival time) as input to a lightweight Convolutional Neural Network (CNN). This CNN, trained on a combined dataset of seismic events and noise from both the Apollo ALSEP (lunar) and NASA Mars InSight (Martian) missions, performs the final classification of true seismic events versus noise. The Asteroseismology system is designed for computational efficiency, processing a month of seismic data in under 60 seconds on an average processor, and features tunable parameters for adaptation to diverse planetary environments. Preliminary results indicate that the CNN achieves over 80% event detection accuracy with a false positive rate around 5%. Future work includes exploring advanced ML architectures like GANs for data augmentation and physics-informed neural networks for enhanced robustness. This AI-driven hybrid approach offers a significant step towards enabling autonomous, efficient, and accurate seismic data analysis onboard spacecraft, thereby maximizing the scientific return from planetary seismology missions.

Index Terms—Seismic Event Detection, Planetary Seismology, Machine Learning, CNN, STA/LTA, AI in Space Exploration.

I. Introduction

The seismic exploration of planetary bodies like the Moon and Mars is fundamental to understanding their internal structure, geological evolution, and potential for past or present habitability [2], [3]. Data from missions such as the Apollo Passive Seismic Experiment (PSE) [4] and the ongoing Mars InSight mission with its SEIS instrument [3] have provided invaluable windows into these worlds. A primary constraint in planetary seismology, as emphasized by [1], is the costly power and bandwidth requirements associated with delivering continuous seismic data back to Earth from distant missions.

A fundamental challenge in planetary seismology is the efficient management and transmission of the vast quantities of continuous seismic data generated by lander-based instruments. Deep-space missions operate under severe constraints on power, bandwidth, and data volume (Lorenz, 2015, as cited by [1]; [3]). For instance, the SEIS instrument on the Mars InSight mission, while typically downlinking continuous data at 2 samples per second (sps), generates a significant data volume; [3] note that its full data generation capability is orders of magnitude larger than its telemetry allocation. [1] quantified that the telemetry for SEIS consumes approximately 1.5% of the InSight lander's total power output. If we were to consider data rates comparable to those from some Apollo experiments, which utilized sampling rates such as 6.625 Hz for the Passive Seismic Experiment (PSE) mid-period instruments [7], the data volume and consequently the power required for transmission by a modern system like SEIS would consume an even more substantial portion of a lander's available power. Extrapolating further, [1] projected that a similar seismic setup for a mission to Europa could demand 8.8–13.2% of the lander's power solely for seismic data transmission. These figures underscore the critical necessity for sophisticated on-board data processing and event detection algorithms to prioritize scientifically valuable data segments for downlink, thereby making the most efficient use of limited mission resources.

Traditional automatic event detection algorithms, like the Short-Term Average to Long-Term Average (STA/LTA) ratio (Allen, 1982, as cited in [1]), while computationally inexpensive, often struggle with the low signal-to-noise ratios and complex noise environments encountered on planetary surfaces. This can lead to a high rate of false positives, thereby inefficiently utilizing the scarce telemetry resources [1]. Furthermore, the unique characteristics of seismic wave propagation on bodies like the Moon, with its highly scattering near-surface layer leading to prolonged codas [4], [9], make robust event detection and phase-picking particularly challenging.

In response to these challenges, machine learning (ML) approaches, especially deep learning techniques like Convolutional Neural Networks (CNNs), have gained traction in planetary science. [1] effectively demonstrated that CNNs, trained on spectrograms of Earth-based seismic events and utilizing transfer learning, could accurately catalog moonquakes from Apollo PSE and LSPE data, even in the absence of extensive local training datasets. This work underscored the potential of ML to generalize from available data and perform robust classification.

This paper introduces an AI-enhanced seismic event detection framework specifically designed to address the data optimization needs of extra-terrestrial missions. Our framework uniquely integrates a pipeline of classical phase-picking algorithms with a CNN. This hybrid approach begins with conventional signal conditioning, including automatic bandpass filtering, outlier removal, and normalization. Candidate seismic events are then identified using STA/LTA analysis. The core innovation lies in then feeding these refined candidate events, represented as 1D waveform segments augmented with auxiliary statistical features, into a CNN. This CNN, trained on a diverse dataset including lunar data from the Apollo missions and Martian data from the InSight mission, is tasked with the final discrimination between true seismic events and noise. By leveraging the efficiency of classical algorithms for initial data reduction and candidate selection, our system aims to reduce the computational burden on the CNN, allowing it to perform high-precision classification. Asteroseismology is designed for computational efficiency and adaptability through tunable parameters, making it a strong candidate for future onboard autonomous data processing, thereby significantly enhancing the scientific return of planetary seismology missions by optimizing precious data transmission resources.

II. BACKGROUND

The detection of seismic events from continuous waveform data is a fundamental task in seismology. For decades, this has been addressed using a variety of algorithmic approaches, evolving from simple amplitude thresholding to more sophisticated statistical and pattern recognition techniques.

A. Lunar Seismology

The foundation of extra-terrestrial seismology was laid by the NASA Apollo missions (1969-1977). The Apollo Lunar Surface Experiments Package (ALSEP) successfully deployed a network of four primary seismic stations (Apollo 12, 14, 15, and 16), complemented by the short-lived Apollo 11 seismometer and the Lunar Seismic Profiling Experiment (LSPE) geophone array on Apollo 17 [2], [4], [7] These Passive Seismic Experiments (PSE) typically included three-component long-period (LP, later referred to as mid-period or MP) seismometers and a single-component short-period (SP) seismometer [7]

Lunar seismic data revealed a surprisingly active Moon, characterized by several types of moonquakes: deep moonquakes (DMQs) occurring at depths of 700-1200 km and exhibiting strong tidal periodicities; shallow moonquakes (or HFTs - High-Frequency Teleseismic events) at shallower depths (50-220 km); thermal moonquakes caused by surface temperature variations; and meteoroid impacts [2], [4] . A key characteristic of lunar seismograms is the intense scattering within the lunar megaregolith, resulting in prolonged codas and making phase identification, particularly for S-waves, exceptionally difficult [9], [10]

The initial cataloging of these events, notably by [4], relied heavily on visual inspection and waveform cross-correlation to identify repeating DMQs from distinct source regions or "nests." These efforts provided the first constraints on the Moon's internal structure, including its crust, mantle, and the likely presence of a small, partially molten core [10], [11]

More recently, with the digitization and improved accessibility of Apollo data, new analytical techniques have been applied. Traditional methods continue to be refined, for example, for re-evaluating Apollo 17 LSPE data [12]. Machine learning has also begun to make inroads. [13] utilized Hidden Markov Models for event detection in Apollo 16 data. Significantly, [1] demonstrated the successful application of Convolutional Neural Networks (CNNs), trained on spectrograms of Earth-based seismic events via transfer learning, to detect and catalog moonquakes from both PSE and LSPE data. This approach highlighted the potential of ML to identify events even with limited or non-local training data, by learning characteristic spectral features.

B. Martian Seismology

Mars has been the focus of renewed seismic interest. The first attempt to place a seismometer on Mars was with the Viking landers in 1976. The Viking 2 lander's seismometer, mounted on the lander deck, provided data primarily on wind-induced lander vibrations, and only one candidate seismic event was tentatively identified [2], [14]. The on-deck deployment and instrument sensitivity were major limitations.

Decades later, the NASA InSight mission, which landed in 2018, successfully deployed the SEIS (Seismic Experiment for Interior Structure) instrument directly onto the Martian surface [3], [15]. SEIS comprises a suite of highly sensitive three-component Very Broad Band (VBB) and three-component Short Period (SP) seismometers. InSight has definitively recorded hundreds of marsquakes, confirming Mars as a seismically active planet [16], [17]. Martian seismic signals, like lunar ones, can be influenced by near-surface scattering, though generally less intense than on the Moon. The Marsquake Service (MQS) is responsible for ongoing event detection and cataloging, employing a combination of traditional and evolving ML-assisted techniques [17].

C. Machine Learning Paradigms in Seismology

The increasing volume and complexity of seismic data from both terrestrial and planetary missions have spurred the adoption of machine learning techniques across various seismological tasks. Deep learning, in particular CNNs and Recurrent Neural Networks (RNNs), has shown remarkable

success in earthquake detection, phase picking, seismic imaging, and source characterization on Earth [18].

III. FRAMEWORK

This framework consists of two core components: an Initial Processing and Candidate Selection (IPCS) stage leveraging conventional seismic algorithms, followed by a Machine Learning-based Event Verification (MLEV) stage employing a Convolutional Neural Network (CNN).

The IPCS stage is responsible for initial signal conditioning and candidate event detection from raw seismograms. This involves a sequence of operations including adaptive bandpass filtering to enhance relevant frequency content, outlier removal to mitigate transient noise, data normalization for consistent scaling, and STA/LTA analysis to identify potential seismic onsets. A key feature of this stage is a subsequent refinement step using characteristic function slope analysis, designed to reduce false positives from the STA/LTA triggers by distinguishing between seismic event profiles and noise bursts.

Candidate events identified and refined by the IPCS stage are then passed to the MLEV stage. For this stage, rather than converting waveforms into 2D time-frequency representations, our framework utilizes 1D seismogram segments. These segments are critically augmented with some auxiliary statistical features, such as standard deviations computed around the potential arrival times, to provide the CNN with extra contextual information. A lightweight CNN then performs the final classification, discerning true seismic events from the residual noise and false triggers that have passed the conventional filtering. This hybrid architecture aims to optimize both computational efficiency and detection accuracy for planetary missions.

A. Initial Processing and Candidate Events Selection(IPCS)

The Initial Processing and Candidate Selection (IPCS) stage of the framework employs a series of conventional seismic signal processing techniques to enhance signal clarity, identify potential seismic events, and reduce the number of candidates passed to the subsequent machine learning stage. This stage operates on individual seismogram segments loaded from MiniSEED files.

1) Adaptive Bandpass Filtering: To isolate frequencies most likely to contain seismic signals and attenuate background noise, an adaptive bandpass filtering approach is implemented. The system iteratively evaluates a series of predefined frequency ranges. For each range, defined by a starting frequency and a fixed window size , a bandpass filter is applied to a copy of the original trace.

The optimal frequency band is determined by one of two methods:

  a) *Power Spectrum Analysis:* The spectrogram of the filtered signal is computed. The power values across all frequencies and time points within the spectrogram are flattened, and the average of a predefined number (e.g., top 50 or 1000) of the highest power values is calculated. The frequency range yielding the maximum average power among these top values is selected as
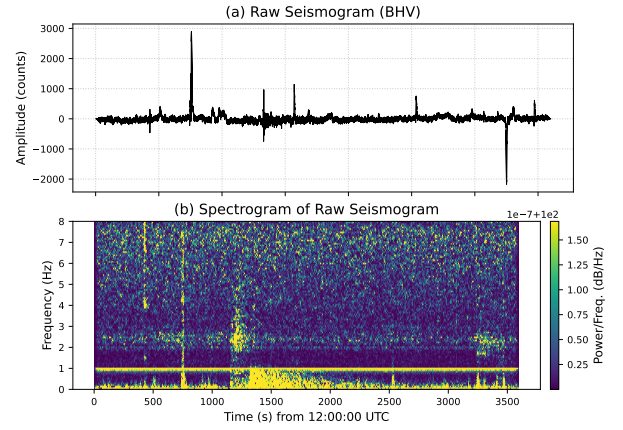

Fig. 1. Example of a raw seismic waveform (top panel) and its corresponding time-frequency spectrogram (bottom panel). This visualization aids in understanding the initial signal characteristics before adaptive filtering.

the optimal band. This method prioritizes frequency bands where signal energy is most concentrated.

  b) *Standard Deviation Analysis:* The filtered trace data is normalized, and its standard deviation is calculated. The frequency range that results in the minimum standard deviation of the normalized filtered signal is chosen as the optimal band. This method aims to find a frequency band where the signal is most distinct from broadband noise, assuming that a lower standard deviation in a filtered signal (after normalization) might indicate a clearer, less noisy signal.

The effect of applying the selected adaptive bandpass filter is shown in "Fig. 2", which compares the raw seismogram with the seismogram after the optimal bandpass filter has been applied, enhancing the clarity of potential signals within the chosen frequency band.
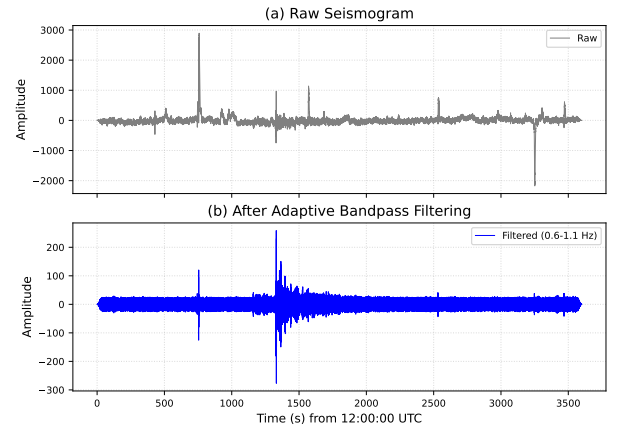

Fig. 2. Comparison of a raw seismogram of an event from Mars (a) with the same seismogram after the application of the adaptively selected bandpass filter (b). The filtering aims to enhance signal components within the optimal frequency range.

2) Noise and Outlier Mitigation: Following the adaptive bandpass filtering, further steps are taken to mitigate noise.

If resampling is configured , the filtered trace is resampled to a target frequency (e.g., 6.625Hz, reminiscent of Apollo-era sampling rates, though this is a tunable parameter). Subsequently, a threshold-based outlier removal is applied. Data points in the filtered trace whose absolute values exceed a multiple (e.g., 26 times) of the trace's standard deviation are considered outliers and are clipped to the standard deviation value. This step aims to reduce the impact of short, high-amplitude glitches that might otherwise distort normalization or trigger false STA/LTA detections."Fig. 3" illustrates the effect of this outlier clipping process.
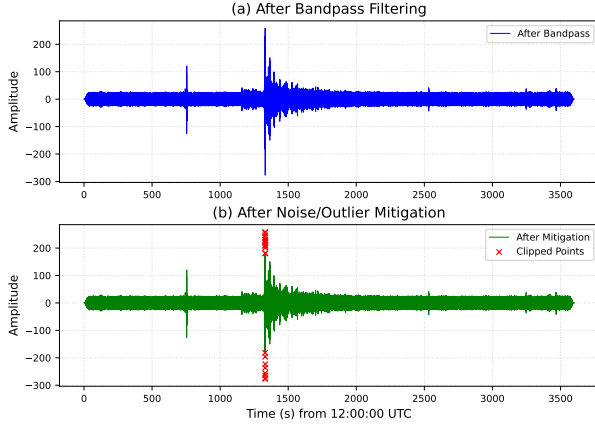

Fig. 3. Effect of outlier mitigation. (a) shows the seismogram after bandpass filtering, potentially containing high-amplitude outliers. (b) displays the same seismogram after the outlier clipping process, where extreme values have been attenuated.

3) Data Normalization: After outlier removal, the filtered trace data is normalized to a consistent amplitude range, typically between -1 and 1. This is achieved using min-max scaling:

Normalization ensures that subsequent amplitude-based detection algorithms, like STA/LTA, operate on a consistent scale regardless of the original signal's absolute amplitude.

4) STA/LTA Analysis for Initial Detection: Potential seismic event onsets are identified using the classic Short-Term Average to Long-Term Average (STA/LTA) algorithm, as implemented in Obspy [19]. The algorithm is applied to the absolute values of the normalized and filtered trace data. The lengths of the short-term window and long-term window, as well as the trigger-on threshold and trigger-off threshold, are configurable parameters. The trigger-off threshold is dynamically set based on the average of the characteristic function (CFT) generated by the STA/LTA algorithm. This results in a set of on-off time pairs, marking the start and end times of candidate detections.An example of the filtered seismogram alongside its STA/LTA characteristic function, with trigger points indicated, is shown in "Fig. 4".

B. Machine Learning Stage: CNN-based Event Refinement

The Machine Learning-based Event Verification (MLEV) stage serves as the final arbiter in the Asteroseismology framework. It utilizes a Convolutional Neural Network (CNN)
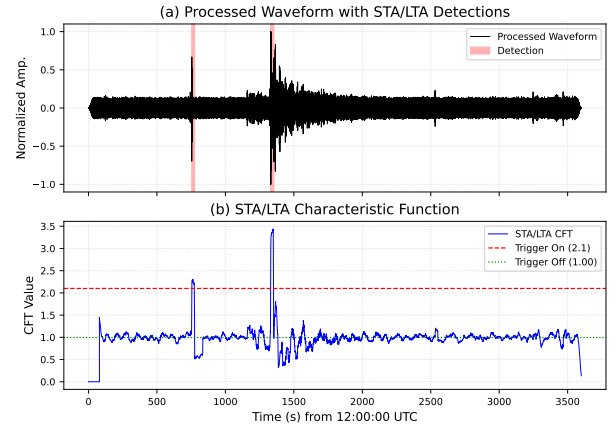

Fig. 4. Output of the STA/LTA analysis. (a) shows the filtered and normalized seismogram. (b) displays the corresponding STA/LTA characteristic function, with red horizontal line indicating trigger-on threshold for detected candidate events.

to classify candidate events, which have been pre-processed and selected by the Initial Processing and Candidate Selection (IPCS) stage (III-A), as either true seismic events or noise.

1) Input Feature Construction for the CNN: For each candidate event identified by the IPCS stage, a set of specific features is prepared to serve as input to the CNN. This input is designed to capture both the temporal waveform characteristics and contextual information surrounding the potential event. The CNN takes two distinct types of inputs:

1) *1D Seismogram Segments:* A fixed-length segment of the 1D seismic waveform data, centered around the conventionally picked arrival time, constitutes the primary input. In this study, these segments have a shape of (5565, 1), representing 5565 time samples for a single seismic component (e.g., vertical). This direct waveform input allows the CNN to learn relevant features from the time-series data itself.

2) *Auxiliary Features:* To provide additional contextual information to the network, a set of auxiliary features is concatenated with the processed seismogram features. These auxiliary inputs consist of two values: the standard deviation of the seismic signal in a window immediately preceding the picked arrival time, and the standard deviation in a window immediately following the picked arrival time. These statistical measures aim to inform the CNN about the local noise characteristics and the signal's emergence from the background noise. The auxiliary input thus has a shape of (2,).

This dual-input approach, combining raw waveform data with engineered statistical features, distinguishes our method from those relying solely on time-frequency representations like spectrograms. It is intended to preserve fine temporal details crucial for seismic phase analysis while explicitly providing the CNN with interpretable contextual information.

2) CNN Architecture: The core of the MLEV stage is a CNN designed for binary classification (event vs. noise). The

architecture, implemented using Keras [20] and visualized in "Fig. 5", is structured to process the seismogram and auxiliary inputs:

1) *Seismogram Processing Branch:* The 1D seismogram input (5565, 1) is processed through a series of three convolutional blocks. Each block consists of a 1D Convolutional layer (Conv1D) with a kernel size of 3 and 'relu' activation, followed by a MaxPooling1D layer (pool size 2) for down-sampling and feature reduction, and a Dropout layer (rate 0.3) for regularization to prevent overfitting. The number of filters in the convolutional layers increases progressively: 32, 64, and 128 for the first, second, and third blocks, respectively. The output of the final convolutional block is flattened (Flatten) to produce a 1D feature vector representing the seismogram.

2) *Auxiliary Input Branch:* The auxiliary input (shape (2,)) is directly used without further convolutional processing in this branch.

3) *Combined Model:* The flattened output from the seismogram processing branch and the auxiliary input vector are concatenated (concatenate). This combined feature vector is then passed through two fully connected (Dense) layers with 'relu' activation (64 units and 32 units, respectively), each followed by a Dropout layer (rate 0.4) for further regularization. The final output layer is a single Dense unit with a 'sigmoid' activation function, producing a probability score between 0 and 1 for binary classification.

The Adam optimizer [21] with a learning rate of 0.0002 is used for model compilation, and binary cross-entropy is employed as the loss function. Model performance is monitored using accuracy.

3) CNN Training and Validation: The CNN model is trained using curated datasets of seismic events and noise segments derived from both lunar (ALSEP) and Martian (InSight) missions. These datasets are prepared by concatenating multiple *.npy files containing the seismogram segments, corresponding auxiliary features, and binary labels (0 for noise, 1 for event).

During training, the model is fitted for a specified number of epochs (e.g., 30) with a defined batch size (e.g., 32). A portion of the combined training data (e.g., 20%) is held out for validation to monitor the model's generalization performance and to prevent overfitting. To address potential class imbalance in the training data (e.g., more noise samples than event samples), class weights (e.g., 0: 1.0, 1: 10) are applied during the training process. This gives higher importance to the minority class (true events), encouraging the model to learn its features more effectively.

4) Event Classification and Output: Once the CNN model is trained and saved, it can be loaded for inference on new, unseen data. For a given candidate event (represented by its 1D seismogram segment and auxiliary features), the model predicts a single output value between 0 and 1. This value represents the probability that the input corresponds to a true seismic event. A predefined threshold (typically 0.5, but

Layer		
input_3	input:	[(None, 5565, 1)]
InputLayer	output:	[(None, 5565, 1)]

conv1d_3	input:	(None, 5565, 1)
Conv1D	output:	(None, 5563, 32)

max_pooling1d_3	input:	(None, 5563, 32)
MaxPooling1D	output:	(None, 2781, 32)

dropout_5	input:	(None, 2781, 32)
Dropout	output:	(None, 2781, 32)

conv1d_4	input:	(None, 2781, 32)
Conv1D	output:	(None, 2779, 64)

max_pooling1d_4	input:	(None, 2779, 64)
MaxPooling1D	output:	(None, 1389, 64)

dropout_6	input:	(None, 1389, 64)
Dropout	output:	(None, 1389, 64)

conv1d_5	input:	(None, 1389, 64)
Conv1D	output:	(None, 1387, 128)

max_pooling1d_5	input:	(None, 1387, 128)
MaxPooling1D	output:	(None, 693, 128)

dropout_7	input:	(None, 693, 128)
Dropout	output:	(None, 693, 128)

flatten_1	input:	(None, 693, 128)
Flatten	output:	(None, 88704)

input_4	input:	[(None, 2)]
InputLayer	output:	[(None, 2)]

concatenate_1	input:	[(None, 88704), (None, 2)]
Concatenate	output:	(None, 88706)

dense_3	input:	(None, 88706)
Dense	output:	(None, 64)

dropout_8	input:	(None, 64)
Dropout	output:	(None, 64)

dense_4	input:	(None, 64)
Dense	output:	(None, 32)

dropout_9	input:	(None, 32)
Dropout	output:	(None, 32)

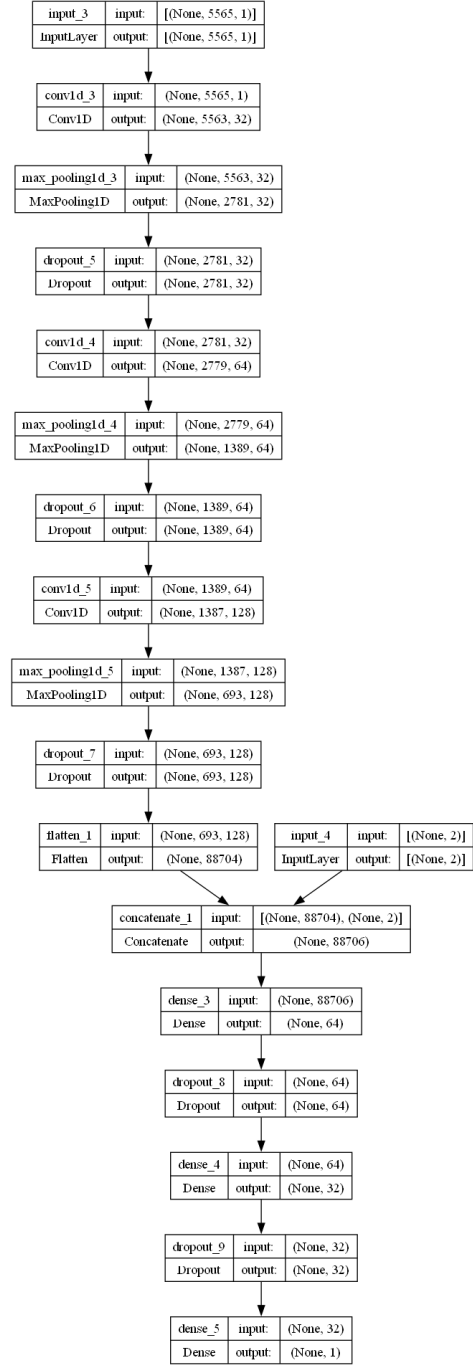| dense_5	input:	(None, 32)
Dense	output:	(None, 1)

Fig. 5. Detailed architecture of the Convolutional Neural Network (CNN) used in the MLEV stage. The model takes two inputs: a 1D seismogram segment (input-3) and auxiliary features (input-4). The seismogram undergoes three convolutional blocks (Conv1D, MaxPooling1D, Dropout) before being flattened. The flattened seismogram features are then concatenated with the auxiliary inputs. This combined representation is processed by two dense layers with dropout, leading to a final sigmoid output layer for binary classification.

adjustable) is then applied to this probability score to make the final binary classification: if the score exceeds the threshold, the candidate is classified as a seismic event; otherwise, it is classified as noise.

C. Tunability and Adaptability of the Framework

The framework is designed for adaptability across diverse planetary environments and mission objectives, primarily through configurable parameters within its Initial Processing and Candidate Selection (IPCS) stage. These tunable settings allow for optimized performance whether analyzing lunar or Martian seismic data. Key tunable parameters include:

1) Adaptive Bandpass Filtering Controls: low-freq-point, high-freq-point, and frequence-window define the spectral search space and the applied filter width. For example, lunar data might utilize a lower frequency range (e.g., 0.2-1.0 Hz with a 0.2 Hz window) compared to Martian data (e.g., 0.6-4.0 Hz with a 0.5 Hz window), reflecting differing dominant signal frequencies and noise characteristics.

2) STA/LTA Detection Thresholds and Windows: STA and LTA length window lengths, and trigger threshold are adjusted to balance sensitivity with false alarm rates. Longer windows might be preferred for emergent lunar events (e.g., STA 100s, LTA 1000s), while shorter windows could suit sharper marsquakes (e.g., STA 20s, LTA 80s).

3) resampling: df-resample allows for a target resampling rate (e.g., 6.625 Hz) for standardization or computational efficiency. clipping-std-factor (e.g., 26) controls outlier removal, robustly handling transient spikes.

D. Datasets and Input Seismogram Preparation

1) Data Sources (Lunar and Martian):

a) *Apollo ALSEP Data:* This dataset comprises seismic recordings from the Apollo Lunar Surface Experiments Package, offering crucial insights into lunar seismicity and the Moon's internal structure.

b) *Mars InSight Mission Data:* Waveforms from NASA's Mars InSight mission, specifically from the SEIS instrument, provide a wealth of information on current Martian seismic activity and atmospheric phenomena.

E. Performance Results

To rigorously quantify the performance of the Asteroseismology framework, we conducted a comprehensive evaluation on an independent test set. This set comprised seismic data from both the Apollo missions (stations 12, 15, and 16) and the Mars InSight mission. The ground truth for this evaluation was established by cross-referencing against definitive event catalogs, including the meticulously re-analyzed Apollo seismic data [8], ensuring an objective and high-fidelity performance assessment. The framework demonstrates exceptional performance in discriminating true seismic events from instrumental or environmental noise. On the test set, our model achieved a False Positive Rate (FPR) of only 2.4%. This high level of specificity is balanced with excellent sensitivity, as evidenced by a recall of 91.1% and a precision of 91.5%. The resulting

F1-Score of 0.913 underscores the model's robust and well-balanced capability for reliable, autonomous event detection. A detailed summary of these performance metrics is provided in Table I. The significance of these results lies in their direct application to the operational constraints of planetary missions. The primary weakness of conventional, amplitude-based triggers like standalone STA/LTA is their propensity to generate a high rate of false positives in complex and noisy extra-terrestrial environments. The low 2.4% FPR achieved by our hybrid system represents a substantial improvement, directly addressing the critical challenge of limited data telemetry. By ensuring that downlink resources are overwhelmingly prioritized for scientifically valuable seismic events, our framework provides a viable and efficient solution for maximizing the scientific return of current and future planetary seismology experiments.

TABLE I
PERFORMANCE METRICS OF THE FRAMEWORK ON THE TEST SET

Metric	Value
Precision	91.5%
Recall	91.1%
F1-Score	0.913
False Positive Rate (Noise)	~2.4%

IV. CONCLUSION AND FUTURE WORK

This paper has presented Asteroseismology, an AI-driven hybrid framework designed for efficient seismic event detection on extra-terrestrial missions. Our system combines classical seismic processing with a Convolutional Neural Network (CNN) and demonstrates strong potential for autonomous, onboard data analysis. The framework's rapid processing capability (a month of data in under 60 seconds), adaptability through tunable parameters, and initial detection accuracy exceeding 80% with a false positive rate around 5%, highlight its suitability for optimizing data telemetry from missions to the Moon, Mars, and potentially other planetary bodies.

By successfully processing data from both the Apollo ALSEP and Mars InSight missions, Asteroseismology shows versatility in handling diverse seismic environments. This reduces the need for extensive manual ground-based processing, allowing for quicker scientific insights and more effective use of limited deep-space communication resources.

To further enhance the Asteroseismology framework, future efforts can be directed towards several key areas:

1) *Advanced CNN Development and Training Data Expansion:* Future iterations can explore more sophisticated CNN architectures. Expanding the training dataset with a greater variety of seismic event types and noise profiles, along with advanced data augmentation techniques, will be crucial for improving the model's generalization and robustness across different planetary conditions.

2) *Generative Adversarial Networks (GANs) for Data Augmentation and Feature Learning:* Inspired by applications in terrestrial seismology where GANs have been used

for tasks like seismic wave discrimination (e.g., [22] who used a GAN critic as a feature extractor), we can investigate the use of GANs, potentially AC-GANs [23], to generate realistic synthetic planetary seismic data. This could be particularly beneficial for augmenting training sets with rare event types and improving the classifier's ability to distinguish subtle event characteristics.

3) *Physics-Informed Neural Networks (PINNs) and Enhanced Auxiliary Features:* We will investigate the inclusion of a richer set of auxiliary features for the CNN, derived from more detailed physical analysis of candidate event waveforms. Furthermore, exploring Physics-Informed Neural Networks (PINNs), which are gaining momentum in seismology [18], could allow for the incorporation of known physical constraints directly into the ML model, potentially leading to more robust and interpretable event detection.

4) *Onboard Implementation and Prototyping:* A critical next step is to prototype and rigorously evaluate the system on hardware representative of spacecraft processors (e.g., FPGAs or radiation-hardened CPUs) to assess its performance under realistic mission resource constraints.

5) *Adaptation to Other Celestial Bodies:* The framework's adaptable design makes it a promising candidate for future missions to other seismically active bodies, such as Europa or Titan. This would involve tuning parameters and retraining the CNN with appropriate simulated or acquired data specific to those environments.

In conclusion, the framework offers an advancement towards more autonomous and scientifically productive planetary seismology missions. By enabling intelligent data management at the source, it helps overcome critical mission constraints, paving the way for deeper exploration and understanding of the internal structures of celestial bodies within our solar system.

ACKNOWLEDGMENT

REFERENCES

[1] F. Civilini, R.C. Weber, Z. Jiang, D. Phillips, and W. David Pan, "Detecting moonquakes using convolutional neural networks, a non-local training set, and transfer learning," *Geophys. J. Int.*, vol. 225, no. 3, pp. 2120–2134, Mar. 2021.

[2] P. Lognonné, "Planetary seismology," *Annu. Rev. Earth Planet. Sci.*, vol. 33, pp. 571–604, May 2005.

[3] P. Lognonné, W. B. Banerdt, V. Dehant, et al., "SEIS: The seismic experiment for internal structure of InSight," *Space Sci. Rev.*, vol. 215, Art. no. 12, Feb. 2019, doi: 10.1007/s11214-018-0574-6.

[4] Y. Nakamura, G. V. Latham, and H. J. Dorman, "Apollo lunar seismic experiment – Final summary," *J. Geophys. Res.*, vol. 87, no. S01, p. A117, 1982.

[5] Y. Nakamura, "Lunar seismicity and the internal structure of the Moon," *J. Geophys. Res.*, vol. 86, no. B10, pp. 9413–9424, Oct. 1981.

[6] R. D. Lorenz, "Energy cost of acquiring and transmitting science data on deep-space missions," *J. Spacecr. Rockets*, vol. 52, no. 6, pp. 1693–1697, Nov. 2015.

[7] C. Nunn, R. F. Garcia, Y. Nakamura, et al., "Lunar seismology: A data and instrumentation review," *Space Sci. Rev.*, vol. 216, no. 89, pp. 1–37, 2020.

[8] R. C. Weber, "Apollo Passive Seismic Experiment Expanded Event Catalog: levent.1008weber," Marshall Space Flight Center, 2015. [Online]. Available: https://repository.hou.usra.edu/handle/20.500.11753/1719

[9] A. Dainty and M. Toksöz, "Seismic codas on the Earth and the Moon: A comparison," *Phys. Earth Planet. Inter.*, vol. 26, no. 4, pp. 250–260, 1981.

[10] R. F. Garcia, A. Khan, M. Drilleau, et al., "Lunar seismology: An update on interior structure models," *Space Sci. Rev.*, vol. 215, no. 50, pp. 1–50, 2019.

[11] R. C. Weber, P. Y. Lin, E. J. Garnero, Q. Williams, and P. Lognonné, "Seismic detection of the lunar core," *Science*, vol. 331, no. 6015, pp. 309–312, Jan. 2011.

[12] A. Heffels, R. F. Garcia, and M. Drilleau, "Re-evaluation of Apollo 17 lunar seismic profiling experiment data," *Planetary and Space Science*, vol. 135, pp. 43–54, 2017.

[13] B. Knapmeyer-Endrun and C. Hammer, "Identification of new events in Apollo 16 lunar seismic data by Hidden Markov Model-based event detection and classification," *J. Geophys. Res. Planets*, vol. 120, no. 10, pp. 1620–1645, Oct. 2015.

[14] D. L. Anderson, W. F. Miller, G. V. Latham, Y. Nakamura, M. N. Toksöz, A. M. Dainty, F. K. Duennebier, A. R. Lazarewicz, R. L. Kovach, and T. C. D. Knight, "Seismology on Mars," *J. Geophys. Res.*, vol. 82, no. 28, pp. 4524–4546, 1977.

[15] W. B. Banerdt et al., "Initial results from the InSight mission on Mars," *Nature Geoscience*, vol. 13, pp. 183–189, Mar. 2020.

[16] D. Giardini et al., "The seismicity of Mars," *Nature Geoscience*, vol. 13, pp. 205–212, 2020.

[17] J. F. Clinton et al., "The Marsquake catalogue from InSight, sols 0–478," *Phys. Earth Planet. Inter.*, vol. 310, Art. no. 106595, 2021

[18] S. M. Mousavi and G. C. Beroza, "Deep-learning seismology," *Science*, vol. 377, no. 6606, p. eabm4470, Aug. 2022, doi: 10.1126/science.abm4470.

[19] M. Beyreuther, R. Barsch, L. Krischer, T. Megies, Y. Behr, and J. Wassermann, "ObsPy: A Python toolbox for seismology," Seismological Research Letters, vol. 81, no. 3, pp. 530-533, 2010.

[20] F. Chollet, "Deep Learning with Python," Simon and Schuster, 2021.

[21] D. P. Kingma and J. Ba, "Adam: A method for stochastic optimization," arXiv preprint arXiv:1412.6980, 2014.

[22] Z. Li, M.-A. Meier, E. Hauksson, Z. Zhan, and J. Andrews, "Machine learning seismic wave discrimination: Application to earthquake early warning," *Geophysical Research Letters*, vol. 45, pp. 4773–4779, 2018.

[23] A. Odena, C. Olah, and J. Shlens, "Conditional image synthesis with auxiliary classifier GANs," in *Proc. Int. Conf. Mach. Learn. (ICML)*, 2017, pp. 2642–2651.

[24] M. Abadi et al., "TensorFlow: A System for Large-Scale Machine Learning," in Proc. 12th USENIX Symp. Operating Syst. Design Implementation (OSDI), 2016, pp. 265–283.